

# Influences of external forcing changes on the summer cooling trend over East Asia

Bian He · Qing Bao · Jiandong Li · Guoxiong Wu ·  
Yimin Liu · Xiacong Wang · Zhaobo Sun

Received: 5 November 2011 / Accepted: 14 September 2012  
© Springer Science+Business Media Dordrecht 2012

**Abstract** Observations indicate a surface cooling trend during the East Asian summer in recent decades, against a background of global warming. This cooling trend is re-examined using station data from 1951 to 2007, and atmospheric general circulation model (AGCM) simulations are performed to investigate the possible influence of changes in external forcing. The numerical experiments are designed to investigate the effects of four types of external forcing: greenhouse gases (GHGs), Total Solar Irradiance (TSI), ozone, and the direct effects of aerosols. Results indicate that external forcing contributes to the cooling trend over East Asia. Furthermore, GHGs, and to a lesser degree the direct effects of aerosols, are the main contributors to the cooling trend. The possible linkages between the external forcings and the cooling trend are discussed.

## 1 Introduction

Climate change in East Asia has been intensively studied in recent decades. Of note, a significant cooling trend in the central parts of East Asia has been reported (Fig. 2b in Menon et al. 2002). Zhou and Huang (2003) demonstrated an association between the cooling trend and changes in precipitation (known as “southern flood and northern drought”) during recent decades over East Asia.

Observational studies have revealed that climate change in East Asia is linked to global warming (Hu et al. 2003) and increasing of aerosols (Xu et al. 2006). Other studies have shown that internal forcing is a mechanism of climate change in the region (Wang et al. 1981).

---

**Electronic supplementary material** The online version of this article (doi:10.1007/s10584-012-0592-4) contains supplementary material, which is available to authorized users.

B. He · Z. Sun  
College of Atmospheric Science, Nanjing University of Information Science & Technology,  
Nanjing 210044, China

B. He · Q. Bao (✉) · J. Li · G. Wu · Y. Liu · X. Wang  
LASG, Institute of Atmospheric Physics, Chinese Academy of Sciences, Beijing 100029, China  
e-mail: baoqing@mail.iap.ac.cn

Recent studies have proposed two mechanisms of external forcing related to surface air temperature (SAT): (1) a straightforward mechanism in which aerosols absorb and scatter solar radiation, with negative shortwave radiative forcing associated with cooling at the surface (Qian et al. 2003); and (2) a relatively indirect mechanism in which surface air temperature changes are attributed to precipitation induced by East Asian Summer Monsoon (EASM), which is influenced by different types of external forcing fields. Some studies have proposed that aerosols can enhance EASM through their influence on circulation, which can result in excessive rainfall (Li et al. 2007). Other studies have reported that the major components of EASM circulation have shown a southward shift during the past 60 years, and monsoonal precipitation in the region has been strongly enhanced by increasing concentrations of greenhouse gases (GHGs) (Li et al. 2010; Yang et al. 2012a).

However, few studies have explored the contributions of external forcing to the cooling trend over East Asia. In this work, we re-examine the observed cooling trend by analyzing extended station datasets, and perform simulations using an AGCM to investigate (1) whether changes in external forcing contribute to the cooling trend over East Asia during summer, and (2) which types of external forcing, if any, are the major contributors to the cooling trend.

The remainder of this paper is organized as follows. Section 2 presents the observational data and the model employed. Section 3 describes the forcing datasets and the experimental design, and Section 4 presents the simulation results and explores the causes of the surface cooling. Finally, a summary of the findings and a discussion on future study of climate change over East Asia are provided in Section 5.

## 2 Observations and model

### 2.1 Observational datasets

The boreal summer cooling trend over East Asia, as identified for the period 1951–2000 (Menon et al. 2002), is further examined in this study based on up-to-date observation data from 714 stations in China. Data are from the China Meteorological Administration (CMA) for the period 1951–2007. The station data show an evident cooling trend (Fig. 1a) and

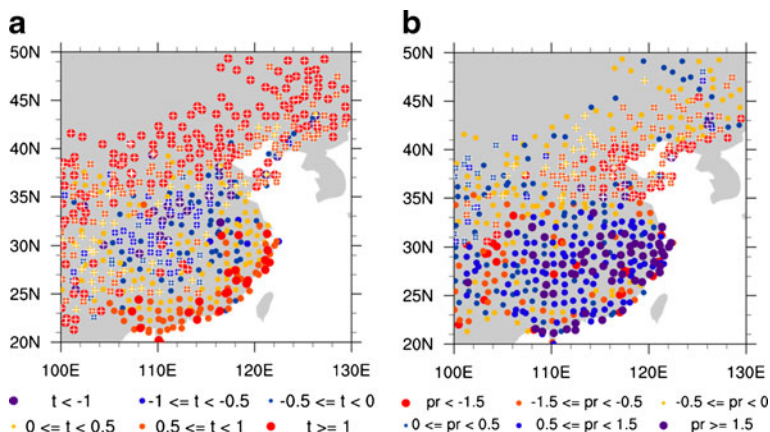


**Fig. 1** Linear trends for the observed June–August (JJA) surface air temperature (a) (unit:  $^{\circ}\text{C}/57$  yrs) and precipitation (b) (unit:  $\text{mmd}^{-1}/57$  yrs) from 1951 to 2007. “+” indicates the linear trends are statistically significant at the 5 % level (Student’s *t*-test)

enhanced precipitation (Fig. 1b) in the central East China region, revealing a strong correlation between changes in temperature and precipitation over the past six decades.

## 2.2 Introduction to the AGCM

The model used in this study is the Spectral Atmospheric Model of LASG/IAP (known as SAMIL) (Bao et al. 2010a), and the land component of SAMIL is NCAR CLM3 (Oleson et al. 2004). The detail description of SAMIL is in an online supplemental material.

SAMIL is commonly used in studies of climatic change over East Asia, and is able to capture the major features of EASM (Duan et al. 2008; Bao et al. 2010b; Yang et al. 2012b). For the topic we discuss here, SAMIL can reproduce the basic spatial pattern of the SAT linear trend over East Asia during summer, whereas the up-to-date Multi Model Ensembles (MME) from the Coupled Model Intercomparison Project phase 5 (CMIP5) coupled models cannot (the detail is also in the online supplemental material).

## 3 Forcing data and experimental design

### 3.1 Forcing data

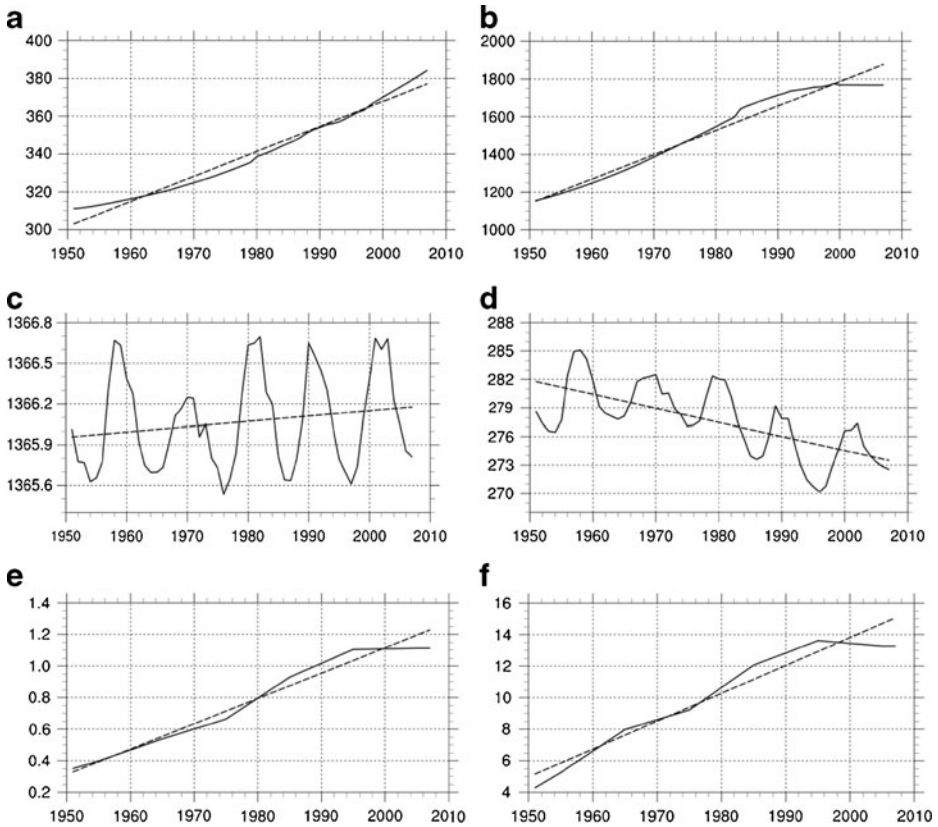
The forcing data used in the AGCM were derived from CMIP5. Monthly mean historical SST and sea ice data from 1948 to 2007 are adopted (Hurrell et al. 2008). The time series of TSI (annual mean values) is derived from Fröhlich and Lean (2004). The other forcing datasets include the annual mean GHGs, such as CO<sub>2</sub>, CH<sub>4</sub>, N<sub>2</sub>O, CFC11, and CFC12 (Buhaug et al. 2009); the monthly mean ozone (Cionni et al. 2011); and the decadal mean aerosols that are linearly interpolated to monthly mean values, including sulfate, black carbon, organic carbon, sea salt, and dust (Lamarque et al. 2010).

Figure 2 shows the time series and linear regressions of external forcings used in the model over East Asia. From 1951 to 2007, the data show increases of 24.83 % in CO<sub>2</sub> content, 69.91 % for CH<sub>4</sub> content, and 328.3 % (black carbon) and 195.01 % (sulfate) for aerosols in total column loading. Ozone content (in DU) decreased by 2.98 % over the same period, and the value of TSI increased by 0.02 %. GHGs and aerosols show a roughly linear increase from 1951 to 2007 (Fig. 2a, b, e, and f), whereas TSI shows no significant trend and the ozone concentration shows a decreasing trend.

### 3.2 Experimental design

Six groups of numerical experiments are performed including one control run (CTL\_RUN) and five sensitivity runs (Table 1). The boundary conditions in all experiments are from the real-time monthly SST and sea ice data. In CTL\_RUN, all the external forcings (including GHGs, TSI, ozone, aerosols) are fixed to the values at 1948. The integration is carried out from 1948 to 2007. Since the radiation budget at the top of model reaches an equilibrium state after 3 years' integration, the first 3-year integrations are treated as the spin-up process. Four sensitivity runs are performed with the different time-varying individual forcings (GHGs, TSI, ozone, and aerosols) listed in Table 1, and the fifth sensitivity run is forced with all four time-varying types of external forcing (ALL\_RUN).

The effects of the external forcing are studied from two perspectives. One is a simple, traditional method by which the linear trend of the climate is calculated from the ALL\_RUN experiment. However, since the historical SSTs already contain the signals of other climate



**Fig. 2** Time series (*solid*) and linear trends (*dashed*) for external forcings during 1951–2007. **a** Annual CO<sub>2</sub> volume mixing ratio (unit: ppm). **b** Annual CH<sub>4</sub> volume mixing ratio (unit: ppb). **c** Annual Total Solar Irradiance (unit: W/m<sup>2</sup>). **d** Regional mean (20°–50°N, 100°–130°E) of JJA total ozone (unit: DU). **e** Same region as in (**d**) for JJA black carbon column loading (unit: mg/m<sup>2</sup>). **f** Same region as in (**d**) for JJA sulfate column loading (unit: mg/m<sup>2</sup>)

forcings, the results from this experiment may double the impacts of external forcing. The other method employs the differences between the sensitivity runs and the CTL\_RUN, because given that both involve historical SST forcing, their difference can be considered

**Table 1** Experimental design of the six group runs

	GHGs	TSI	Ozone	Aerosols	SST&SICE
CTL_RUN	Fixed	Fixed	Fixed	Fixed	Time-varying
GHG_RUN	Time-varying	Fixed	Fixed	Fixed	Time-varying
TSI_RUN	Fixed	Time-varying	Fixed	Fixed	Time-varying
OZO_RUN	Fixed	Fixed	Time-varying	Fixed	Time-varying
AER_RUN	Fixed	Fixed	Fixed	Time-varying	Time-varying
ALL_RUN	Time-varying	Time-varying	Time-varying	Time-varying	Time-varying

Fixed: external forcing is fixed at the value in 1948

Time-varying: external forcings evolve from 1948 to 2007

to result mainly from external forcing. A simple linear regression method is used as the main tool in analyzing the SAT change.

## 4 Results

### 4.1 Linear trend in SAT

To evaluate the effects of external forcing over East Asia in recent years, the differences between ALL\_RUN and CTL\_RUN are used to indicate the combined effect of historical GHGs, direct aerosols, ozone, and TSI on climate change over East Asia.

Figure 3a shows the simulated linear trends of summer (JJA) mean SAT caused by the four types of external forcing. The combined effect of external forcings on SAT change during the past 57 years (1951–2007) indicates a minor warming trend, with a mean value of  $0.17\text{ }^{\circ}\text{C}$  over East Asia ( $20^{\circ}$ – $50^{\circ}\text{N}$ ,  $100^{\circ}$ – $130^{\circ}\text{E}$ ) and a global mean value of  $0.31\text{ }^{\circ}\text{C}$ . The spatial pattern of

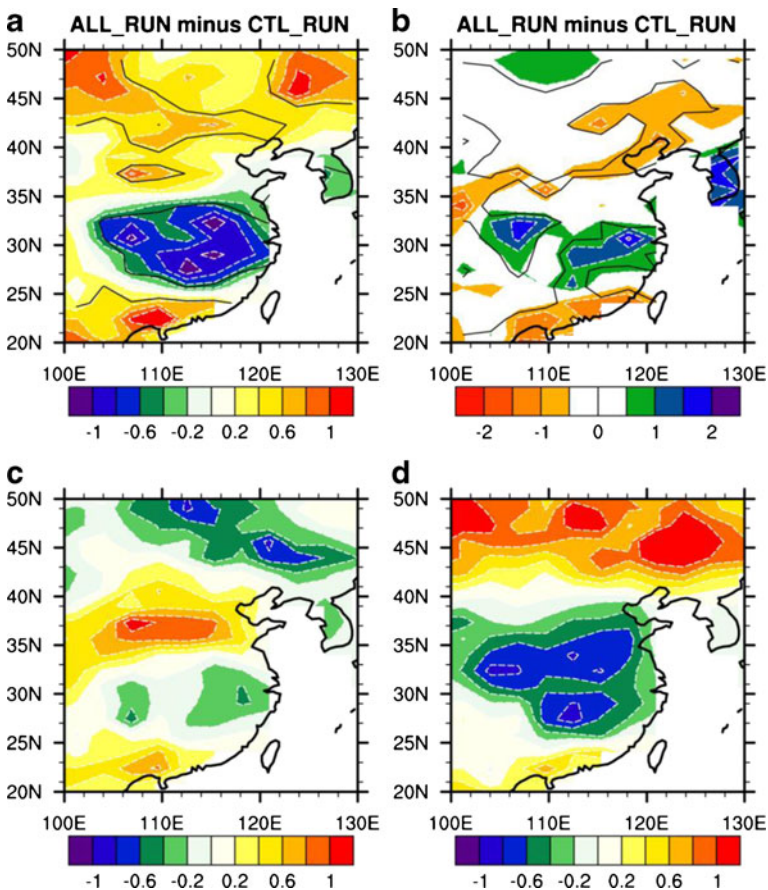


**Fig 3** Linear trends of JJA SAT (unit:  $^{\circ}\text{C}/57\text{ yrs}$ ) (a) and precipitation (unit:  $\text{mm d}^{-1}/57\text{ yrs}$ ) (b) for ALL\_RUN minus CTL\_RUN, and contributions to the total cooling over East China due to external forcing from (c) a linear combination and (d) nonlinear impacts (unit:  $^{\circ}\text{C}/57\text{ yrs}$ ). See the text for details. The black solid lines in (a), (b) are statistically significant at the 5 % level (Student's *t*-test)

cooling and warming trends is similar to that observed (Fig. 1a). The simulation result shows a significant cooling center in central East China, especially along the middle and lower reaches of the Yangtze River, while a clear warming trend appears over northern China. The magnitude of the cooling trend induced by the external forcing is up to  $-0.8\text{ }^{\circ}\text{C}$ , which is also very similar to that derived from the station data. Therefore, our numerical results suggest that the external forcings have contributed to the cooling trend in summer surface temperatures over East Asia.

The simulated precipitation change over the past 57 years appears to be strongly related to SAT change (Fig. 3b), since precipitation shows a robust, positive linear trend over central China (maximum increase of 2 mm/day) and a significant negative trend over northern China. The spatial pattern of simulated precipitation change is similar to that based on the rain-gauge station data (Fig. 1b), indicating that changes in external forcing during recent decadal years have contributed to changes in EASM. This may, to some extent, explain the “southern flood and northern drought” trend.

Moreover, the area with a positive precipitation trend in Fig. 3b comprises two regions: the Sichuan Basin and the downstream area of the Yangtze River, corresponding to the regions of cooling SAT. The cooling trend may be influenced by various forcing fields, with increasing  $\text{SO}_2$  concentrations considered the main contributor to cooling in the Sichuan Basin during recent decades (Li et al. 1995), and atmospheric circulation anomalies being the main contributor to excessive rainfall along the Yangtze River. Therefore, it is important to examine which of the external forcings is the dominant control on the cooling trend over central China. Below, we present the results of simulations that individually consider GHGs, TSI, ozone, and aerosols, and we discuss the possible causes through which these forcings influence the surface cooling over East Asia.

We consider four scenarios that are each perturbed by a sole external forcing (Table 1), and estimate the atmospheric response to the specific external forcing by calculating the difference between each scenario and CTL\_RUN. The experimental design does not consider some of the nonlinear interactions among these external forcings due to atmospheric motion.

Figure 4 shows the linear response of SAT to the four separate forcings. A cooling trend for SAT is present over central China for all four scenarios, with relatively robust responses in the GHGs scenario (Fig. 4a) and the aerosols scenario (Fig. 4c). A weak cooling trend appears in the ozone scenario (Fig. 4d) over southern China, and warming occurs over northern China. For the TSI scenario (Fig. 4b), the SAT cooling trend is not statistically significant. Therefore, TSI and ozone may not be the major contributors to East Asian summer cooling patterns.

A comparison of the total effects of all types of external forcing (Fig. 3a) with the effects of individual forcings (Fig. 4) shows a much stronger SAT cooling response. This indicates that the nonlinear interactions among these forcings may play an important role in the surface cooling over East Asia. To further examine this point, we assume that the total forced trend  $\Delta T_{ALL}$  can be divided into a linear part  $\Delta T_{linear}$  and a nonlinear part  $\Delta T_{nonlinear}$ ; i.e.,

$$\Delta T_{ALL} = \Delta T_{linear} + \Delta T_{nonlinear}.$$

The linear part can be obtained as

$$\Delta T_{linear} = \lambda_1 * \Delta T_{linear}^{GHGs} + \lambda_2 * \Delta T_{linear}^{TSI} + \lambda_3 * \Delta T_{linear}^{Aerosols} + \lambda_4 * \Delta T_{linear}^{Ozone}, \text{ in which } \lambda_1 + \lambda_2 + \lambda_3 + \lambda_4 = 1.$$

To obtain the weighted coefficients  $\lambda_1$ ,  $\lambda_2$ ,  $\lambda_3$ , and  $\lambda_4$ , we add the cooling amounts in Fig. 4 that are significant over the region ( $25^{\circ}$ – $35^{\circ}\text{N}$ ,  $105^{\circ}$ – $120^{\circ}\text{E}$ ) for each of the

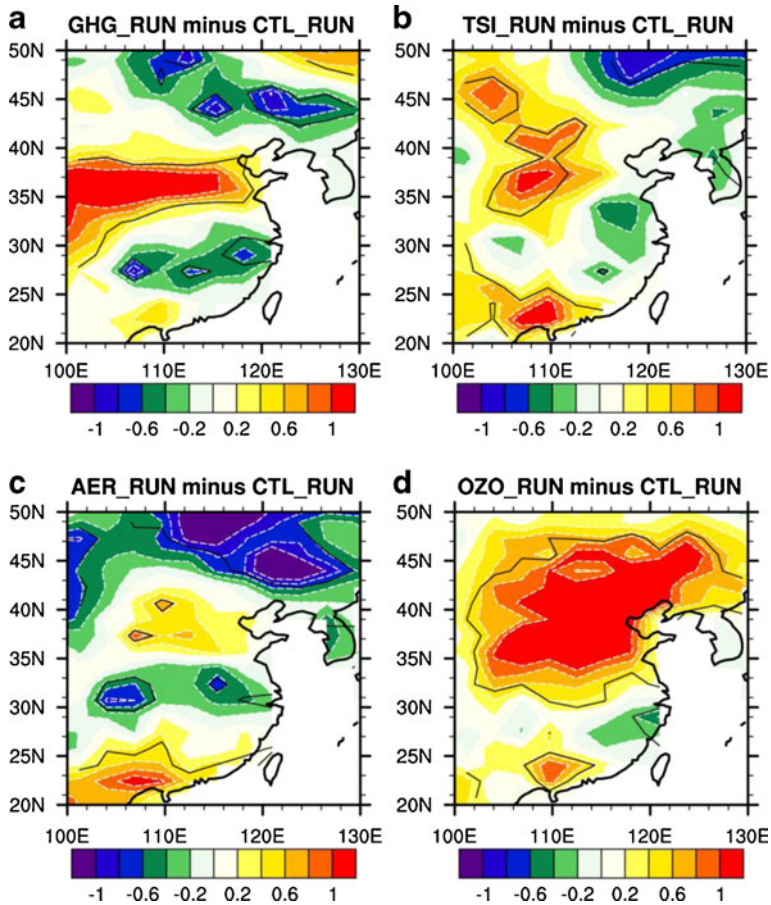


**Fig. 4** Linear trends for JJA SAT for the four difference scenarios (unit: °C/57 yrs): **a** GHG\_RUN minus CTL\_RUN; **b** TSI\_RUN minus CTL\_RUN; **c** AER\_RUN minus CTL\_RUN; and **d** OZO\_RUN minus CTL\_RUN. The *solid lines* are statistically significant at the 5 % level (Student’s *t*-test)

experiment results. After normalizing the four total cooling values, we have

$$\lambda_1 = 0.429, \lambda_2 = 0.078, \lambda_3 = 0.379, \lambda_4 = 0.114.$$

Thus, the effects of the linear part  $\Delta T_{linear}$  are calculated and shown in Fig. 3c. By using  $\Delta T_{nonlinear} = \Delta T_{ALL} - \Delta T_{linear}$ , the effects of nonlinear interactions of the external forcings are calculated and shown in Fig. 3d. A comparison of Fig. 3c and d with Fig. 3a shows that both the linear and nonlinear impacts contribute to the cooling over the central East China, with the nonlinear impacts dominating the cooling trends.

#### 4.2 Possible causes of the cooling trend

The effect of external forcings on the summer cooling trend over East Asia is shown to be important in Fig. 3a; however, to diagnose which of the external forcings acts as the dominant control is difficult using ALL\_RUN minus CTL\_RUN, since the land, ocean, and atmospheric interactions are all combined within the model. Therefore, it is important to use the individual

scenarios, particularly GHGs and aerosols (the two major contributors), to diagnose the possible cause of the cooling trend and to understand the physical process in a simplified way.

In the GHG scenario, the JJA SAT trends show warming almost globally, particularly in the Northern Hemisphere (figure not shown), but there exists an obvious cooling trend over East Asia (Fig. 4a) accompanied by increasing precipitation (Fig. 5a). This indicates that the surface atmospheric response may have a close relationship with the variation of the EASM.

An important response to changes in GHGs is the change of the hydrological cycle (Held and Soden 2006). According to the Clausius–Clapeyron expression, variations in the saturated water vapor are in proportion to the changes in temperature. The total column water vapor in the atmosphere would increase by 7.5 % with a surface air temperature increase of 1 K. In our study, total column water vapor shows a significant increase over southern parts of East Asia (Fig. 5b), in accordance with the spatial distribution of SAT cooling (Fig. 4a) and increased precipitation (Fig. 5a).

Increasing water vapor not only leads to intensified precipitation, but also has an impact on cloud fraction change and radiation feedback over land. The simulated total cloud

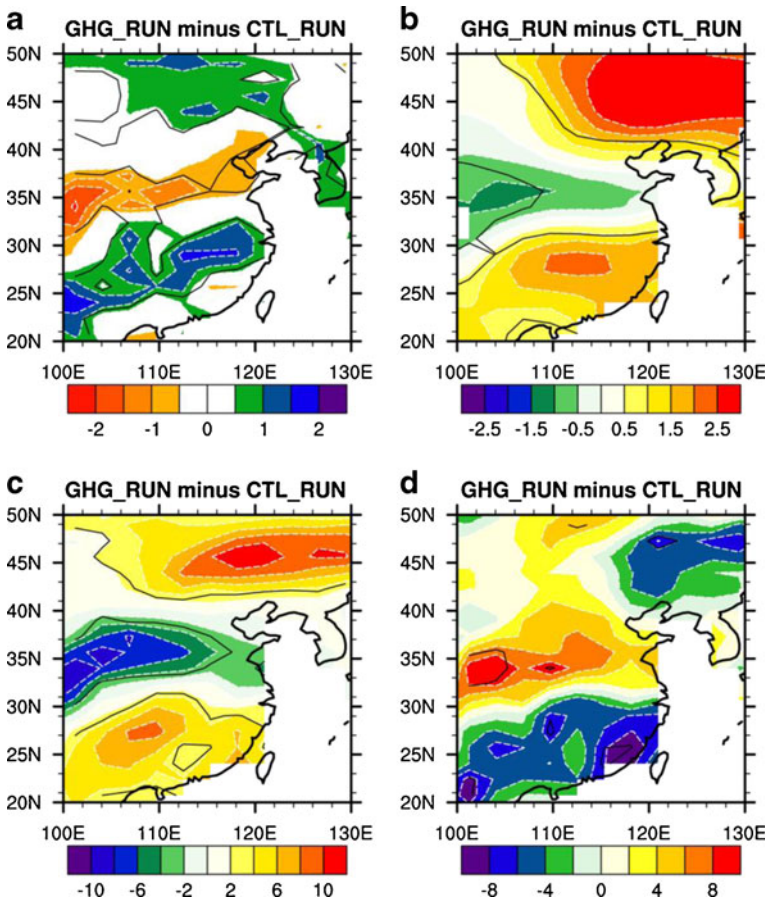


**Fig. 5** Linear trends for June–August (JJA) in GHG\_RUN minus CTL\_RUN using (a) precipitation (unit:  $\text{mm d}^{-1}/57$  yrs); (b) total column water vapor (unit:  $\text{kg m}^{-2}/57$  yrs); (c) total cloud fraction (unit:  $\%/57$  yrs); and (d) net radiation at surface (unit:  $\text{W m}^{-2}/57$  yrs). The *solid lines* are statistically significant at the 5 % level (Student's *t*-test)

fraction change (Fig. 5c) shows a remarkable similarity to the change in water vapor, increasing by 4 %–8 % over Southern China. On the other hand, the increasing precipitation will also lead to an intensification of latent heat flux in situ (figure not shown), and the cool the surface through the evaporation process.

All of these factors have an impact on the net surface radiation budget. The increasing amounts of water vapor and cloud cover absorb more shortwave radiation in the atmosphere, and the evaporation take heat from the ground into the atmosphere, leading to a net surface radiation decrease in Southern China (Fig. 5d), which may be a cause of the cooling trend in this region.

As another important external forcing, aerosols may play a different role to that of GHGs in causing the cooling trend in SAT. The aerosols forcing fields that are time-varying during the integration show a rapid increase over East Asia in recent decades (Fig. 2e,f). Meanwhile, the low level temperature in this area is increasing in AER\_RUN minus CTL\_RUN (figure not shown), by given that the black carbon could absorb solar radiation and heat the atmosphere (Ramanathan and Carmichael 2008) and the maximum of black carbon locate over northern China (Fig. 6a), we infer black carbon may play a more important role in

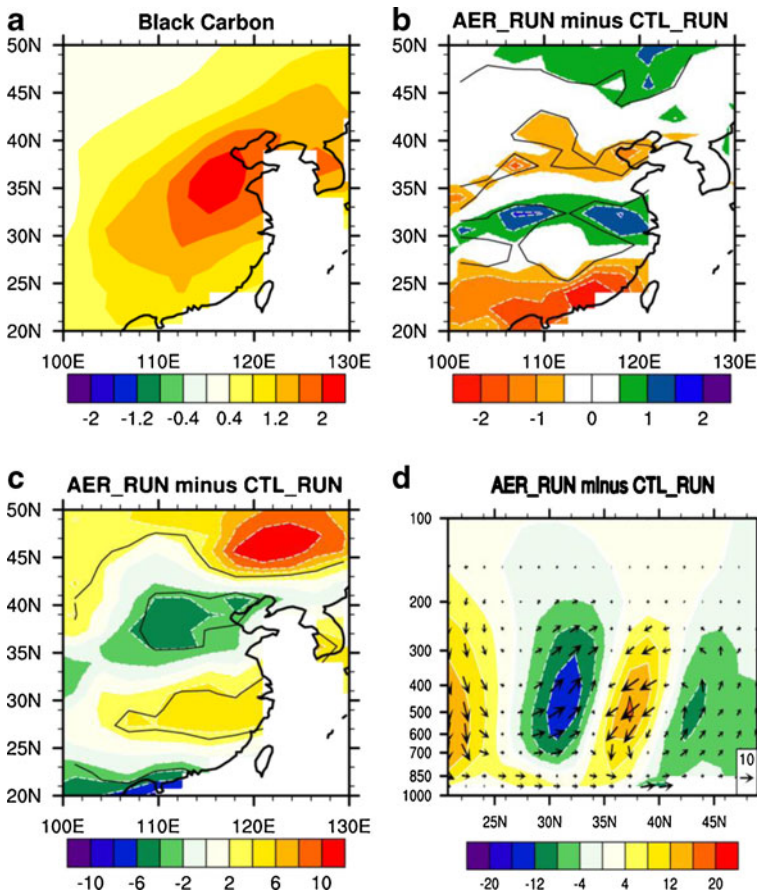


**Fig. 6** Linear trends for June–August (JJA) of (a) total column black carbon (unit:  $\text{mgm}^2/57 \text{ yrs}$ ) and in AER\_RUN minus CTL\_RUN, (b) precipitation (unit:  $\text{mm d}^{-1}/57 \text{ yrs}$ ), (c) total cloud cover ( $\%/57 \text{ yrs}$ ), and (d) averaged vertical velocity along 105°–120°E (shaded, unit:  $10^{-3} \text{ Pa s}^{-2}/57 \text{ yrs}$ ) and  $v^*(-\omega)$  (vector, unit:  $10^{-3} \text{ Pa m s}^{-2}/57 \text{ yrs}$ ). The solid lines in (b), (c) are statistically significant at the 5 % level (Student’s *t*-test)

this study. The low-level air becomes more stable (figure not shown) and could have an impact on local cloud radiation feedback, meaning that the climate over north China become dryer (Fig. 6b), warmer (Fig. 4c), and less cloudy (Fig. 6c).

However, the linear trend in precipitation (Fig. 6b) shows two significant centers in central China, coincident with the location of the two SAT cooling centers. This result indicates that rainfall induced by aerosols could potentially be the main cause of SAT cooling, in agreement with Menon et al. (2002). Figure 6d shows a cross-section of the vertical velocity along 105°–120°E. When the black carbon heats the air and induces descending motion over 35°N, it also bring more cold air at high levels from the north, which could interact with the low-level warm wet air brought by the East Asia monsoon, thus resulting in enhanced summer monsoon rainfall over the Yangtze River region, potentially resulting in cooler surface temperatures (Fig. 4c).

## 5 Conclusions and discussion

### 5.1 Conclusions

This study aimed to examine the contributions of all types of external forcing (GHGs, TSI, ozone, and aerosols) to the cooling trend in the surface air temperature over East Asia during recent decades. Based on results obtained from the analysis of observational data and AGCM experiments, we arrived at the following conclusions:

- (1) The cooling trend over central China is evident from up-to-date station datasets over an extended period.
- (2) The combined effect of all the external forcings contributes to the SAT cooling trend over the central China, and the region of the enhanced monsoon precipitation corresponds to the region of SAT change.
- (3) The results of sensitivity experiments indicate that nonlinear interactions among external forcings make an important contribution to surface cooling over East Asia. The two major contributors to the cooling trend are GHGs and the direct effect of aerosols.
- (4) The relationship between external forcing changes and the surface cooling trend over central China indicate that increasing GHGs induce global warming, leading to enhanced water vapor in the warming air and more clouds over central and southern China. The East Asian subtropical rain belt is strengthened. This change, coupled with a negative surface radiation balance, results in SAT cooling.
- (5) Aerosols increase in North China, thereby affecting atmospheric stability and bringing more cold air at higher levels from North China to South China, resulting in turn in warm, dry, and less cloudy conditions over North China, and cool, wet, and cloudy conditions over South China.

### 5.2 Discussion

State-of-the-art coupled models have limitations in reproducing climate change, especially over East Asia (Kang et al. 2002). All models, including SAMIL, have bias in their physical processes. To reduce the model bias when performing numerical sensitivity experiments, it's helpful to consider the difference between two experiments based on one model.

The model used here did not consider the indirect effect of aerosols. It remains unclear whether aerosols lead to flood or drought (Rosenfeld et al. 2008), as cloud condensation nuclei (CCN) are not well simulated and the numbers and sizes of aerosols are poorly known; in addition, the dominant control on the indirect effect of aerosols on precipitation (Giorgi et al. 2003) or on radiation (Wang et al. 2010) remains a topic of controversy. Despite these uncertainties, indirect effects have an important impact on the East Asian climate (Cheng et al. 2005). Aerosols can alter the physical and micro-physical characteristics of clouds, thereby affecting solar radiation forcing and precipitation over East Asia (Huang et al. 2006; Qian et al. 2009). In fact, Lohmann and Feichter (2005) argued that the indirect effect of aerosols may be more important than their direct effect. Therefore, it is necessary to examine the indirect effect of aerosols on the cooling trend over central China in future.

Another important forcing field not considered in the present analysis is land cover change over East Asia during the study period. The latest research has indicated that land use/land cover change (LULCC) represents a first-order anthropogenic climate forcing, as it affects surface latent heating, sensible heating, regional radiative heating, and moisture convergence (Mahmood et al. 2010). In terms of East Asia, previous studies have reported that the EASM and its vertical structure are affected by large-scale LULCC (Wang et al. 2006). Zhang et al. (2005) also studied the possible impacts of land use change on surface temperature over China, in terms of changes to the surface energy balance and the hydrological cycle. Taken together, these findings indicate that decadal-scale variability in SAT is sensitive to changes in LULCC over China. To simulate the impact of LULCC, a higher-resolution model is required.

The two main anthropogenic emissions over East Asia, carbon and sulfate, affect climate change in different ways (Huang et al. 2008; Wu et al. 2009; Liu et al. 2010), making it necessary to investigate the contributions and interactions of different types of aerosols individually.

Furthermore, because the simulations performed here employed prescribed SST data, part of the effect induced by external forcing is already included in the AMIP run, and ocean–atmosphere feedbacks are only considered in the atmospheric response. The experiment design used here has, to some extent, removed the possible duplication of external forcings.

However, a state-of-the-art coupled model would still be essential to enable a more meaningful evaluation of the contributions of external forcing to evaporation over oceans, surface net radiation, and the hydrological cycle in the climate system (Ramanathan 1981). In this regard, the results here can be considered a reference framework for comparison with future results from coupled runs.

Finally, the climate change pattern over East Asia (Wet/cool in the south and dry/warm in the north) has been studied extensively, and has been attributed to changes in SST (Zhou et al. 2009) and Tibetan Plateau forcing (Liu et al. 2012; Wu et al. 2012). Thus, the external forcing discussed here should be considered as just one of multiple contributors, and their relative importance should be analyzed in further studies.

**Acknowledgements** This study was supported by ‘973’ programs (Grant Nos. 2012CB417203, 2013CB955803, 2010CB950404), CAS Strategic Priority Research Program (Grant No. XDA05110303), the National Science Foundation of China (Grant Nos. 41023002), and the Postgraduate Innovation Program of Jiangsu China (Grant No. N0782002054).

## References

- Bao Q, Wu G, Liu Y, Yang J, Wang Z, Zhou T (2010a) An introduction to the coupled model FGOALS1.1-s and its performance in East Asia. *Adv Atmos Sci* 27(5):1131–1142
- Bao Q, Liu YM, Shi JC, Wu GX (2010b) Comparisons of soil moisture datasets over the Tibetan Plateau and application to the simulation of Asian Summer Monsoon onset. *Adv Atmos Sci* 27(2):303–314
- Buhaug et al. (2009) Second IMO GHG study 2009. International Maritime Organization (IMO) London UK
- Cheng YJ, Lohmann U, Zhang JH et al (2005) Contribution of changes in Sea Surface Temperature and aerosol loading to the decreasing precipitation trend in southern China. *J Climate* 18:1381–1390
- Cionni I, Eyring V, Lamarque JF et al (2011) Ozone database in support of CMIP5 simulations: results and corresponding radiative forcing. *Atmos Chem Phys Discuss* 11:10875–10933. doi:10.5194/acpd-11-10875-2011
- Duan AM, Wu GX, Liang XY (2008) Influence of the Tibetan Plateau on the summer climate patterns over Asia in the IAP/LASG SAMIL model. *Adv Atmos Sci* 25(4):518–528
- Fröhlich C, Lean J (2004) Solar radiative output and its variability: evidence and Mechanisms. *Astron Astrophys Rev* 12(4):273–320. doi:10.1007/s00159-004-0024-1
- Giorgi F, Bi XQ, Qian Y (2003) Indirect vs direct effects of anthropogenic sulfate on the climate of East Asia as simulated with a regional coupled climate-chemistry/aerosol model. *Clim Chang* 58:345–376
- Held IM, Soden BJ (2006) Robust responses of the hydrological cycle to global warming. *J Climate* 19:5686–5699
- Hu ZZ, Yang S, Wu R (2003) Long-term climate variations in China and global warming signals. *J Geophys Res* 108(D19):4614. doi:10.1029/2003JD003651
- Huang Y, Dickinson RE, Chameides WL (2006) Impact of aerosol indirect effect on surface temperature over East Asia. *Proc Natl Acad Sci* 103(12):4371–4376
- Huang Y, Chameides WL, Tan Q, Dickinson RE (2008) Characteristics of anthropogenic sulfate and carbonaceous aerosols over East Asia: regional modeling and observation. *Adv Atmos Sci* 25(6):946–959
- Hurrell JW, Hack JJ, Shea D, Caron JM, Rosinski J (2008) A new sea surface temperature and sea ice boundary dataset for the community atmosphere model. *J Climate* 21:5145–5153
- Kang IS et al (2002) Intercomparison of the climatological variations of Asian summer monsoon precipitation simulated by 10 GCMs. *Clim Dyn* 19:383–395
- Lamarque JF, Bond TC, Eyring V et al (2010) Historical (1850–2000) gridded anthropogenic and biomass emissions of reactive gases and aerosols: methodology and application. *Atmos Chem Phys* 10:7017–7039. doi:10.5194/acp-10-7017-2010
- Li XW, Zhou XJ, Li WL, Chen LX (1995) The cooling of Sichuan Province in recent 40 years and its probable mechanisms. *Acta Meteorologica Sinica* 9(1):57–68
- Li LJ, Wang B, Zhou TJ (2007) Contributions of natural and anthropogenic forcing to the summer cooling over eastern China: an AGCM study. *Geophys Res Letts* 34:L18807
- Li JP, Zhu ZW, Jiang ZH, He JH (2010) Can global warming strengthen the East Asian Summer monsoon? *J Climate* 23:6696–6705. doi:10.1175/2010JCLI3434.1
- Liu HN, Zhang L, Wu J (2010) A modeling study of the climate effects of sulfate and carbonaceous aerosols over China. *Adv Atmos Sci* 27(6):1276–1288
- Liu YM et al (2012) Revisiting Asian monsoon formation and change associated with Tibetan Plateau forcing: II. Change. *Clim Dyn*. doi:10.1007/s00382-012-1335-y
- Lohmann U, Feichter J (2005) Global indirect aerosol effects: a review. *Atmos Chem Phys* 5:715–737
- Mahmood R et al (2010) Impacts of land use/land cover change on climate and future research priorities. *Bull Am Meteorol Soc* 91(1):37–46
- Menon S, Hansen J, Nazarenko L, Luo Y (2002) Climate effects of black carbon aerosols in China and India. *Science* 297:2250–2252
- Oleson KW et al (2004) Technical description of the community land model (CLM). NCAR/TN-461 + STR
- Qian Y, Leung LR, Ghan SJ, Giorgi F (2003) Effects of increasing aerosol on regional climate change in China: Observation and modeling. *Tellus Ser B* 55:914–934
- Qian Y, Gong D, Fan J, Leung LR, Bennartz R, Wang W (2009) Heavy pollution suppresses light rain in China: observation and modeling. *J Geophys Res* 114:D00K02. doi:10.1029/2008JD011575
- Ramanathan V (1981) The role of ocean–atmosphere interactions in the CO<sub>2</sub> climate problem. *J Atmos Sci* 38:918–930
- Ramanathan V, Carmichael G (2008) Global and regional climate changes due to black carbon. *Nat Geosci* 1:221–227
- Rosenfeld D, Lohmann U, Raga GB, O’Dowd CD, Kulmala M, Fuzzi S, Reissell A, Andreae MO (2008) Flood or drought: how do aerosols affect precipitation? *Science* 321:1039–1313
- Wang SW, Zhao ZC, Chen ZH (1981) Reconstruction of the summer rainfall regime for the last 500 years in China. *Geojournal* 5:117–122

- Wang HJ, Shi WL, Chen XH (2006) The statistical significance test of regional climate change caused by land use and land cover variation in West China. *Adv Atmos Sci* 23(3):355–364
- Wang ZL, Zhang H, Shen XS, Gong SL, Zhang XY (2010) Modeling study of aerosol indirect effects on global climate with an AGCM. *Adv Atmos Sci* 27(5):1064–1077
- Wu D et al (2009) Black carbon aerosols and their radiative properties in the Pearl River Delta region. *Sci China Ser D-Earth Sci* 52(8):1152–1163
- Wu GX et al (2012) Thermal controls on the Asian summer monsoon. *Sci Rep* 2:404. doi:[10.1038/srep00404](https://doi.org/10.1038/srep00404)
- Xu M, Chang CP, Fu C, Qi Y, Robock A, Robinson D, Zhang H (2006) Steady decline of East Asian monsoon winds, 1969–2000: evidence from direct ground measurements of wind speed. *J Geophys Res* 111: D24111. doi:[10.1029/2006JD007337](https://doi.org/10.1029/2006JD007337)
- Yang J, Bao Q, Wang X (2012a) Intensified eastward and northward propagation of tropical intraseasonal oscillation over equatorial Indian Ocean in global warming scenario. *Adv Atmos Sci*. doi:[10.1007/s00376-012-1260-3](https://doi.org/10.1007/s00376-012-1260-3)
- Yang J, Bao Q, Wang X, Zhou T (2012b) The tropical intraseasonal oscillation in SAMIL coupled and uncoupled general circulation models. *Adv Atmos Sci* 29(3):529–543. doi:[10.1007/s00376-011-1087-3](https://doi.org/10.1007/s00376-011-1087-3)
- Zhang JY, Dong WJ, Wu LY, Wei JF, Chen PY, Lee DK (2005) Impact of land use changes on surface warming in China. *Adv Atmos Sci* 22(3):343–348
- Zhou LT, Huang RH (2003) Research on the characteristics of interdecadal variability of summer climate in China and its possible cause. *Climatic Environ Res* 8(3):274–290 (in Chinese)
- Zhou TJ, Gong DJ, Li J, Li B (2009) Detecting and understanding the multi-decadal variability of the East Asian Summer Monsoon—recent progress and state of affairs. *Meteorol Z* 18(4):455–467